Research and Reviews in Materials Science and Chemistry
Vol. 2, Issue 1, 2013, Pages 19-60
ISSN 2319-6920
Published Online on March 30, 2013

http://jyotiacademicpress.net

EROSION-CORROSION IN OIL AND GAS PRODUCTION

BAOTONG LU

Department of Materials Engineering
Southwest Research Institute
San Antonio
TX, 78238
USA
e-mail: baotong.lu@swri.org

Abstract

Challenges due to erosion-corrosion in oil and gas production are briefly reviewed. The achievements of the author's group on the modelling of synergistic effects erosion are summarized. The erosion-corrosion mechanisms, the methods to evaluate the erosion-corrosion resistance of materials and the approaches to mitigate the damage caused by erosion-corrosion are discussed in this article.

1. Introduction

With a few exceptions, most metals owe their corrosion resistance to a protective surface film. Erosive fluids can damage the protective film, and remove small pieces of material as well, leading to a significant increase in penetration rate. For instance, carbon steel pipe carrying water is usually protected by a film of rust and its corrosion rates are typically

Keywords and phrases: erosion, corrosion, petroleum, evaluation, mitigation.

Communicated by Qiuming Peng.

Received July 16, 2012; Revised August 16, 2012

< 1mm/y (or 40mils/y). The removal of the film by erosive slurry gives corrosion rates of the order of 10mm/y (400mils/y) in addition to the any erosion of underlying metal [1]. The damage to the protect film may be the results of the fluid-induced mechanical forces or flowing-enhanced dissolution [2, 3]. Meanwhile, the corrosion can cause degradation in surface properties and promote the mechanical erosion under action of the mechanical forces [4]. This conjoint action of erosion and corrosion is known as erosion-corrosion [5]. Erosion-corrosion encompasses a wide range of flow induced corrosion [6]. It is also regarded as a subject within the broader area of tribo-corrosion, which covers all aspects of tribologically (mainly mechanically) induced interactions with electrochemical processes [7]. As summarized by Postlethwaite and Nesic [6], the sources of the various mechanical forces that cause erosion-corrosion include:

(1) Turbulent flow, fluctuating shear stress, and pressure impacts.

(2) Impact of suspended solid particles.

(3) Impact of suspended liquid droplets in high-speed gas flow.

(4) Impact of suspended gas bubbles in aqueous flow.

(5) The violent collapse of vapour bubbles following cavitation.

The five mechanical force sources mentioned above can be found in oil and gas production. The fluids to induce erosion-corrosion may be single phase like the portable water or multiphase flows such as various combinations of gas, oil, water, and solid particles in petroleum industry [8]. It is well known that the turbulent flow, fluctuating shear stress, and pressure impacts are sources of flow accelerated corrosion in pipelines transporting oil and water [9], and the violent collapse of vapour bubbles in pumps and valves can result in cavitation-corrosion [10]. A few typical problems of erosion-corrosion in oil and gas production are specifically mentioned as follows:

● The downhole components. Petroleum and mining drill bits are subjected to highly abrasive rock and high velocity fluid so that erosion-

corrosion is among the most failure mechanisms of downhole components [11]. The entire downhole tubing string is exposed to erosion-corrosion, but points if radical flow diversion or construction such as pumps, downhole screens, chokes, and subsurface safety valves are particularly at risk [12, 13]. In the downholes of gas wells, the erosion-corrosion may result from the impingement of mixture of corrosive liquid droplets [14].

- The systems used to contain, transport and process erosive mineral slurries. This is particularly important for the oil sand industry of northern Alberta, Canada, where handling the processing of essentially silica-based sand (tar sand) results in server erosion-corrosion problems [7, 15].

- With the technique of CO_2 injection for enhanced oil recovery and active exploitation of deep nature gas reservoirs containing CO_2, server corrosion of carbon steel is experienced [16]. In CO_2-saturated environments, the $FeCO_3$ scale may form and it can provide protection to some extent. The sand present in production fluids may damage and/or remove the protective scale, leading to erosion-corrosion [17].

- Petroleum refinery equipment components, typically, pump internals, thermo wells, piping elbows, nozzle, valves seats, and guides, experience varying degrees of high temperature erosion and corrosion. The erosion-corrosion effects are predominant in fluidized catalytic crackers, delayed cokers, flexicokers, thermal crackers, and vacuum distillation units [18]. High temperature crude oil moving with high velocity across the tube wall surface may cause server localized damage. Such kind of damage may be related to the naphethenic acids that are highly aggressive in a temperature range from 220°C to 400°C [19] and the high turbulence of fluid [20, 21]. The material loss is increased significantly by the small amount of fine erodent in the crude oils that are extracted from bitumen of oil sand.

According to a recent survey, erosion-corrosion was rated in the top 5 most prevalent forms of corrosion damage in the oil and gas production

[22] and cause an immense economic loss [23, 24]. Many review articles on topic of erosion-corrosion investigation from different view angles can be found in open literature [3, 6, 7, 23]. In this paper, an attempt will be made to overview the progresses achieved in the evaluation of erosion-corrosion resistance of materials and the mitigation methods. The emphasis will be put on the synergistic effects in erosion-corrosion in flowing slurries.

2. Erosion, Corrosion and their Synergism

The mechanisms of flow accelerated corrosion related to the destructing and reforming of protect films. The protect films fall into two categories: (1) the relative thick porous diffusion barriers, formed on carbon steels (red rust) and copper alloys (cuprous oxide) and (2) the thin invisible passive films on stainless steels, nickel alloy, and other passive metals like titanium [6]. A spectrum of erosion-corrosion process in Table 1 was summarized by Poulson [3, 24]. Actually, this spectrum is more suitable to the metals with loose and less protective surface scale exposed to a single phase flow. The erosion-corrosion mechanisms of passive metals in flowing slurries are much more complicated than those shown in Table 1. For example, the mechanical erosion may contribute a major part of total material loss of stainless steels in marine pumping applications, where solid erodent are present, even under the condition that the protect film is only partially removed [25]. A large amount of experimental data have indicated that, even if the corrosion component is very small, e.g., less than 5% of the pure mechanical erosion rate in absence of corrosion, the resulting erosion-corrosion rate may be much greater than that without corrosion [14, 26, 27, 28, 29, 30]. With implantation of sand production controls, such as gravel-packing completion, the prone reservoirs produce still sand up to 5 pounds per thousand barrels and results in considerable material loss due to erosion-corrosion [12]. Experimental evidence indicated that the corrosion due to wet CO_2 might accelerate the erosion of C-Mn steel by a factor of 2-4

[12]. Because of the damage and removal of protective scale caused by the sand impingement, the corrosion rate also increased significantly [12, 17].

Table 1. Spectrum of erosion-corrosion processes [3, 23]

Electrochemical dissolution dominated	
Mechanism	Erosion-corrosion rate
Flow thins protective film to equilibrium Thickness, which is a function of both mass transfer and growth kinetics.	The metal loss rate is very low and it is controlled by the dissolution of the protective film.
Film is locally removed by dissolution, fluid induced stress or particle/bubble impact and the repassivation occurs simultaneously.	The erosion-corrosion rate is a function of film removal, bare metal dissolution rate and subsequent repassivation rate.
Film is removed and does not reform.	It is equal to the dissolution rate of bare metal.
Film is removed and underlying metal surface is mechanically damaged, which contributes to the overall metal loss.	It is the sum of the dissolution rate of bare metal and the possible synergistic effect of mechanical damage.
Film is removed and mechanical damage to the underlying metal is dominant damage mechanism.	The direct contribution of corrosion is relatively small.
Mechanical damage dominated	

As mentioned above, two different material loss mechanisms are involved in erosion-corrosion of metals, mechanical erosion, and electrochemical corrosion. The mechanical erosion relates to plastic deformation and rupture in surface layer. Small pieces of metal are removed from the surface by various mechanical forces *before* being ionized. The electrochemical corrosion relates to the metal being dissolved into the slurry *after* it is ionized. Therefore, the total material loss rate $\dot{w}$ is the sum of material loss rates caused by erosion $\dot{e}$ and corrosion $\dot{c}$,

$$\dot{w} = \dot{e} + \dot{c}. \tag{1}$$

To be more accurate, the corrosion rate is the more suitable term in the place of 'erosion-corrosion rate' in Table 1. The total material loss of material in corrosive fluids is normally larger than the sum of those caused by pure mechanical erosion and pure electrochemical corrosion.

According to standard of ASTM G119, the pure mechanical erosion is defined as the erosion in an inert environment and the pure electrochemical corrosion is the corrosion under erosion-free condition. The additional wastages of erosion and corrosion components caused by the synergistic effects are regarded as the corrosion-enhanced erosion $\dot{e}_c$ and the erosion-enhanced corrosion $\dot{c}_e$ [31],

$$\dot{e} = \dot{e}_0 + \dot{e}_c; \tag{2}$$

$$\dot{c} = \dot{c}_0 + \dot{c}_e. \tag{3}$$

The erosion-corrosion mechanism is affected by all the factors, which control corrosion and all the factors, which affect erosion. In combination, the damage is synergistic and can be extremely aggressive. The synergism of erosion and corrosion, $\dot{s}$, is expressed as the sum of $\dot{e}_c$ and $\dot{c}_e$ [31]:

$$\dot{s} = \dot{e}_c + \dot{c}_e. \tag{4}$$

The synergism often contributes to such a large part of the total material loss [26, 27, 28, 29, 30, 32, 33, 34], that it cannot be ignored in service lifetime assessment in engineering. The corrosion is erosive liquid can be determined by using the standard procedures that used in erosion-free condition, such as the one to measure the linear polarization resistance (ASTM G59) [35] and the one to generate the potentiodynamic curves (ASTM G5) [36]. The pure mechanical erosion rate in corrosive slurries should be conducted under the same hydrodynamic conditions under cathodic protection. ASTM G119 recommended polarizing the specimen to one volt cathodic with respect to the open circuit potential to guarantee a fully protected condition. However, caution must be taken because hydrogen embrittlement may occur in some materials under the cathodic protection. Besides, the gas bubbles produced by the hydrogen evolution may affect the hydrodynamic conditions. A recent study indicated that the erosion rates under cathodic protection in the slurries prepared by dilute acidic solutions are much higher than those in neutral and alkaline slurries [37]. In line with ASTM G119, the following dimensionless factors can be defined to describe the degree of synergism:

$$\text{Total synergism factor} = \frac{\dot{w}}{\dot{w} - \dot{s}} = 1 + \frac{\dot{s}}{\dot{e}_0 + \dot{c}_0}. \quad (5)$$

$$\text{Corrosion augmentation} = \frac{\dot{c}}{\dot{c}_0} = 1 + \frac{\dot{c}_e}{\dot{c}_0}. \quad (6)$$

$$\text{Erosion augmentation} = \frac{\dot{e}}{\dot{e}_0} = 1 + \frac{\dot{e}_c}{\dot{e}_0}. \quad (7)$$

Although efforts have been made, it is still difficult to build an integral model of erosion-corrosion [38, 39, 40], because a large amount of factors are involved in the erosion-corrosion processes including the metallurgical features of material [41, 42, 43, 44], the hydrodynamics of fluid [45, 46], and flow field [47], the characteristics of erodent [48, 49, 50, 51], the temperature [52, 53], and corrosivity of media [37, 54].

During impingement, the sand degradation may result from the broken of sand particles and/or the bluntness of particle corner or edge, leading to a reduced erosion rate. If the effect of sand degradation is excluded, the erosion rate under a given hydrodynamic condition is independent of time [40, 55]. The total material loss rate resulting from a cavitating liquid or impingement of liquid droplets is a function of time. There is an incubation time within which the rate of material loss is negligible. After the incubation, the material loss rate increases rapidly, reaches a peak value and then reduces to a steady value gradually [56, 57].

3. Corrosion in Fluids

3.1. Corrosion under control of mass transfer at electrode/electrolyte interface

When corrosion is controlled by the mass transfer of dissolved oxygen or in the boundary layer of the liquid at the electrolyte/electrode or diffusion of some other soluble species away from the surface [24], the corrosion rate is formulated as follows [58, 59, 60, 61, 62]:

$$Sh = \alpha Re^{\beta} Sc^{\gamma}. \quad (8)$$

The non-dimensional parameters in Equation (8) are Sherwood number $Sh = Kd/D$, Reynolds number $Re = Ud/\nu$, and Schmidt number $Sc = \nu/D$; where α, β, and γ are constants depending upon the flow conditions and the geometry of the test devices; K is the specific mass transfer coefficient, d is the specific size depending on the geometry of test device; D is the diffusion coefficient of the species of which diffusion in the boundary layer controls the corrosion process; U is the flow velocity; and ν is the kinematic viscosity of the fluid.

Equation (8) was originally established in the rotating disk electrode (RDE) system based on kinetics of electrochemical reaction [63]. When the electrochemical reaction over the RDE surface is mass transfer control, $\alpha = 0.791$, $\beta = 0.7$, and $\gamma = 0.356$. Equation (8) was extended to various systems. In a straight pipe, d in Equation (8) could be the pipe diameter. Corrosion rate $\dot{c} = K\Delta C$, as the corrosion is dominated by the mass transfer process in the boundary layer at the electrode/electrolyte interface. ΔC is the concentration driving force or concentration drop of species within the boundary layer, of which the diffusion controls the corrosion process. Thus,

$$\dot{c} = K\Delta C = \alpha Re^{\beta} Sc^{\gamma} D\Delta C/d = \alpha \Delta C D^{1-\beta} d^{\gamma-1} \nu^{\beta-\gamma} U^{\beta}. \tag{9}$$

Equation (9) has been validated experimentally, such as the test data shown in Figure 1. Dissolved oxygen is often believed to be the species in the flowing electrolyte controlling the corrosion process. If the corrosion reaction at the target surface is solely controlled by the diffusion of dissolved oxygen within the boundary layer, the corrosion rate is proportional to the limited current density $i_{\lim}$ of dissolved oxygen [59, 60, 61, 62] and the corrosion rate $\dot{c}$ is given by

$$\dot{c} = \eta K C_0, \tag{10}$$

where C_0 is the dissolved oxygen concentration in bulk liquid medium. Theoretically, $\eta = 1$. Postlethwaite et al. pointed out only $2/3$ of dissolved oxygen reaching the wall is used in oxidizing the iron into

ferrous ions and that the rest is used in the oxidization of the ferrous ions to ferric ions close to the wall, so that $\eta = 2/3$ [11].

In Figure 1, the exponent determined the flowing tailing water free of solid particle is around 0.75 and that in following slurries is about 0.55. This is because the linear relationship $\dot{c} = K\Delta C$ not always held. Generally, $\dot{c} \propto K^m$ [3, 24]. The deviation of m-value from 1 suggests the corrosion reaction is not fully under the mass transfer control, as depicted in Figure 2 [3, 8, 24]. In the flowing electrolyte free of sand, corrosion scale would form on the target surface ($n > 1$: case 2 in Figure 2). In flowing slurry, the impingement of solid particles would remove the corrosion scale and the activation of electrode may result from the dynamic plastic strain in the surface layer ($n < 1$: case 4 in Figure 2). In real pipe system, the surface roughness can affect the β-value [58, 64]. For a mass transfer-controlled corrosion reaction, the value for β may range from 0.5 to 1 [6].

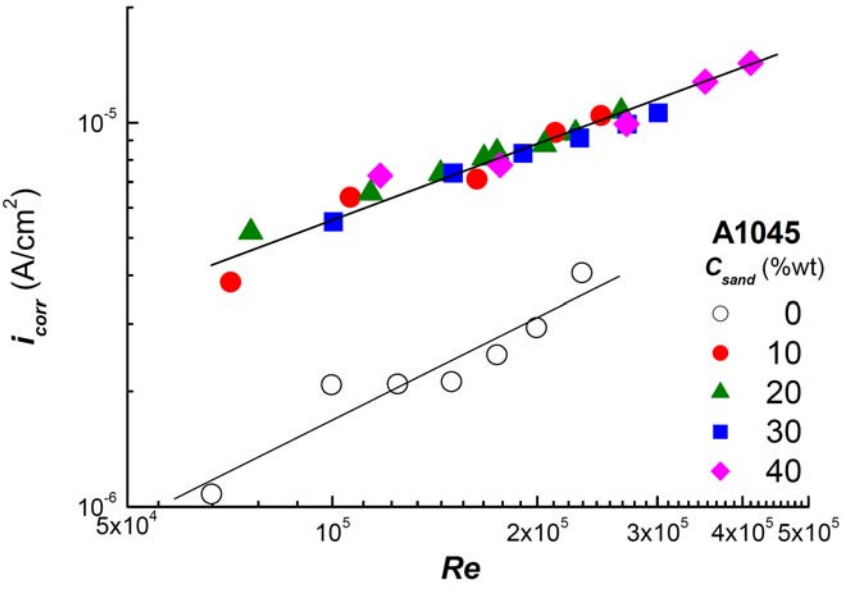

Figure 1. The dependence of corrosion rate on the Reynolds number. (Target material: carbon steel A1045; slurry: tailing water of oil sand production + silica sand, RCE system) 0.55/slurry, 0.75 solution [65].

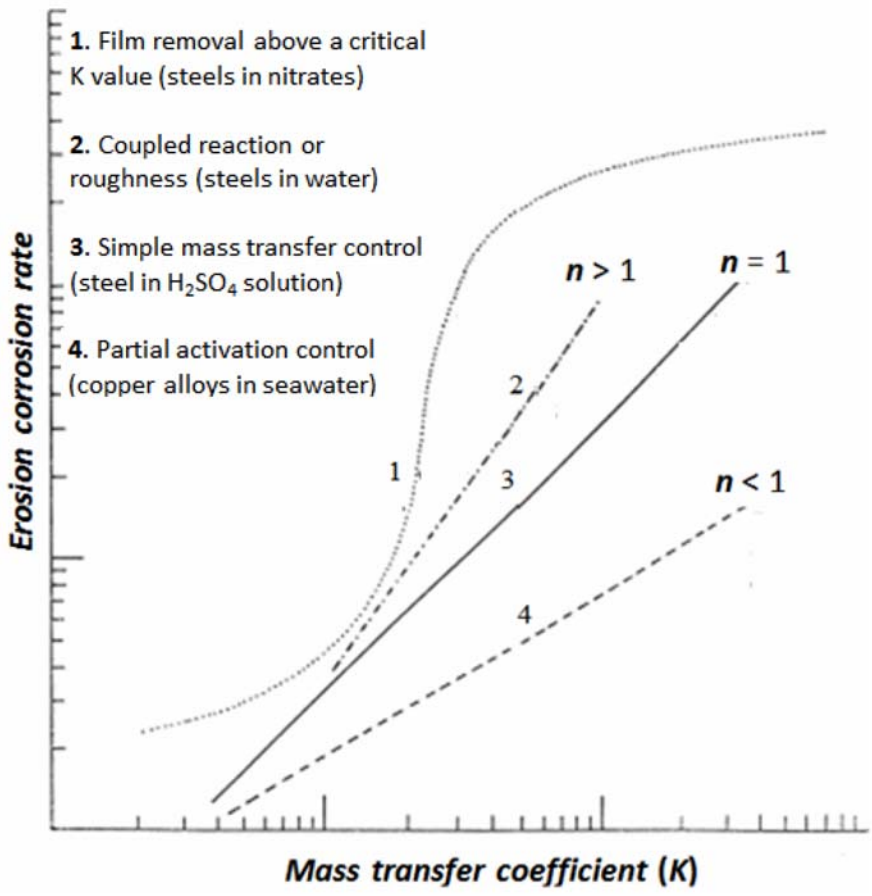

Figure 2. Possible relationship between erosion-corrosion rate and mass transfer [3, 24].

When the protective corrosion product scale exists on the surface, the apparent mass transport coefficient K is formulated as follows [66]:

$$\frac{1}{K} = \frac{1}{K_B} + \frac{1}{K_F}, \tag{11}$$

where K_B and K_F are the mass transport coefficients in the boundary layer and the corrosion product film, respectively. If the metal is under the passive condition, the mass transfer in the passive film will be much

slower than that the liquid phase, $K_B >> K_F$ and $K \approx K_F$. If the fluid does not induce the breakdown of passive film, the corrosion of iron-based alloys is controlled by the diffusion of oxygen vacancy within the passive film [67] and hence the corrosion rate is controlled by the density and diffusion coefficient of oxygen vacancy density within the passive film [68]. If the fluid cannot destroy the passive film, a high flowing velocity can increase the dissolved oxygen supply at the electrode/electrolyte interface, leading to a reduced oxygen vacancy density in the passive film. As a result, the passive current density is likely to be reduced. If the fluid damages and/or destructs the passive film, the corrosion rate will increased dramatically [69].

3.2. Critical impingement velocity

The exact mechanism of protective film damage during erosion-corrosion in single-phased turbulent flow is still in doubt. There is uncertainty regarding the roles of mechanical forces and mass transfer in film disruption since both of them are directly related to turbulence intensity [6]. An industry standard, API RP-14E [70] recommends an empirical formula, originally developed from the experience in electric power industry with erosion-corrosion of carbon steel by steam condensate, to estimate the critical velocity U_e (ft/s) beyond which the corrosion rate will become unacceptable high due to onset of erosion-corrosion

$$U_e = \frac{C_{API}}{\rho_F^{1/2}}, \tag{12}$$

where ρ_F is the density of fluid in Ibft^{-3} and C_{API} is a constant. A constant 450 is recommended for use in seawater injection systems constructed from corrosion-resistant alloys, 100 is for other materials and 150-200 for inhibited systems. The liquid jet impingement tests on API 5CT L80 12Cr steel indicate the erosion-corrosion resistance in absence of solid particle is considerably higher than that predicted by API RP-14E [69]. The critical velocity is also a function of environment and system

geometry [8]. Efforts have been made to modify Equation (8) to provide more universal C_{API} factor, by taking the hardness of surface films into account [71]. Because the protective film (passive film or corrosion product scale) is very thin (~10nm or less), both the theory and experimental techniques for evaluating the mechanical properties of the protective film are not well established [72]. The critical velocity U_e can be regarded as the critical condition leading to passive film breakdown and, therefore, it is useful tool to evaluate the erosion-corrosion susceptibility of materials under impingement liquid droplet suspending in high velocity gas flow [14]. However, it does not relate to the corrosion rate after the passive film breakdown.

3.3. Wall shear stresses

Based on the experimental observation of copper alloy tubes with a diameter of 25mm [73], Efird [74] propose the concept of 'critical wall shear stress' for film disruption

$$\tau_w = \frac{\Delta P}{4x/d} = f\frac{\rho_m U^2}{2}, \tag{13}$$

where f is the Fanning friction factor [75] and its values for pipes with various surface roughness can be obtained from a Moody chart [76]. The concept of critical wall shear stress has been used to evaluate the performance of protective film of inhibitor in CO_2 corrosion of carbon steel [77]. However, this idea was not tested to see if the concept of critical wall shear stress was applicable to other geometries [8]. It has been pointed out that, the wall shear stresses obtained are too low to remove the corrosion product scale from the pipe wall [6, 8, 24, 78].

The most severe erosion-corrosion problems occur under conditions of disturbed turbulent flow at sudden changes on the flowing system, such as bends, heat-exchanger-tube inlets, orifice plates, values, fittings, and in turbo-machinery including pumps, compressors, turbines, and propellers [6]. The experimental evidence indicated that, it is difficult to correlate the corrosion rate in the detached flow produced by the

downstream of pipe expansion to the wall shear stress [24]. In reality, there are fluctuating shear stress and pressure at the wall and the largest values are obtained quasi-cyclic bursting events close to the wall [6]. It is worthy of studying the possibility that the corrosion product scale is physically removed by the stress resulting from the turbulent fluid [24].

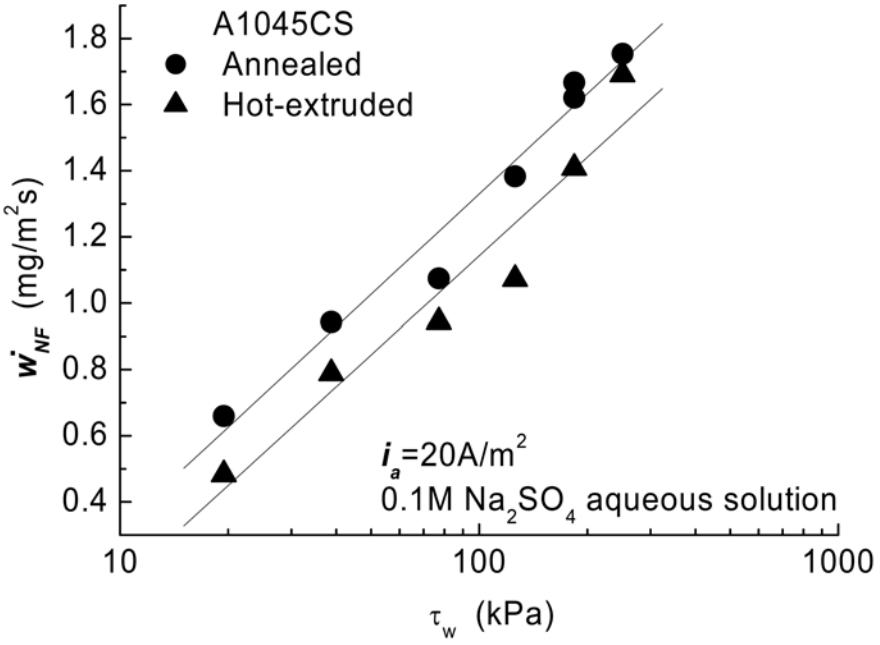

Figure 3. Effect of hardness of target material and wall shear stress on non-Faradaic material loss [79].

In addition to corrosion process in fluid, the wall shear stress may cause an extra material loss in a corroding medium. It was found that the actual material loss in flowing electrolytes free of solid particle measured with weight loss method was higher than that calculated with the Faraday's law based on the anodic current density determined by the electrochemical approach [79, 80]. The extra material loss is defined as non-Faraday's material loss.

$$\dot{w}_{NF} = \dot{w} - \dot{w}_F, \tag{14}$$

where $\dot{w}$ is total material loss measured with the weight loss method and the Faraday's material loss is equal to the corrosion rate

$$\dot{w}_F = \dot{c} = \frac{M}{zF} i_{\text{corr}}. \tag{15}$$

The non-Faraday's material loss disappears as the corrosion is ceased by cathodic protection. However, it increases with increasing anodic current density and the wall shear stress (Figure 3), suggesting it is a result of synergistic effect between the mechanical force and corrosion.

3.4. Corrosion of passive metals in flowing slurry

When the kinetic energy of solid particles in flowing slurry exceeds a threshold value, the particle impingement will remove a small piece of passive film and produce a crater. It will lead to a sharp rise of local corrosion current over the crate surface. Then, the local current will decay with time because of repassivation [81]. As a result, the corrosion current density over target surface that is impacted by slurry is no longer uniform and the average corrosion current density will depends on the rate of passive film removal and repassivation kinetics. In line with the kinetic analysis of slurry impingement, the average current density over the whole electrode surface $\bar{i}$ can be expressed as [82]:

$$\bar{i} = \frac{1}{A}\int_0^A i\,dA = \dot{A}_e \int_0^\infty i \exp\left(-\dot{A}_e t\right) dt, \tag{16}$$

where i is the local current density that is a function of the repassivation kinetics, A is the surface area of target, and $\dot{A}_e \left(= C_p U \sin\theta \overline{A}_{crater} / \overline{m}_p \right)$ is the generation rate of the active surface area caused by slurry impingement. C_p and $\overline{m}_p$ are the concentration (kg/m^3) and average mass (kg) of solid particle, respectively, θ is the impingement angle, $\overline{A}_{crater}$ is the average surface area of crater produced by the individual particle impingement that can be measured from SEM image of surface impacted by the slurry. The kinetic mode and parameters of repassivation depend on the nature of target materials, as well as chemical

characteristics and hydrodynamics of corrosion media, and can be determined directly by using the single particle impingement or scratch test [52, 83]. When the repassivation follows the bi-exponential law, as indicated by 304 stainless steel in the tap water [52],

$$i = i_S + i_1 \exp\left(-\frac{t}{\tau_1}\right) + i_2 \exp\left(-\frac{t}{\tau_2}\right), \tag{17}$$

where the second term in Equation (17) (i_1, τ_1) relates to certain quickly decaying processes such as the formation of a passive film with monolayer thickness on a bared crater surface, and the third term (i_2, τ_2) relates to a slowly decaying process for growth of a passive film [84]; $i_1 + i_2 = i_{peak}$, i_{peak} is the peak response of local current density over the crate surface to the particle impingement; i_S is the stable current density in the flowing water free of sand. In this case, the corrosion current density in flowing slurry is formulated as follows by inserting Equation (17) into Equation (16) and integrating [52]

$$\bar{i} = i_S + i_1 \frac{\lambda_1}{1+\lambda_1} + i_2 \frac{\lambda_2}{1+\lambda_2}. \tag{18}$$

The non-dimensional parameters are $\lambda_1 = \tau_1 \dot{A}_e$ and $\lambda_2 = \tau_2 \dot{A}_e$ that represent the combined effects of the hydrodynamic conditions and repassivation kinetics. An example in Figures 4 and 5 indicate that Equation (18) gives a good prediction to the corrosion current density of 304SS in the flowing slurries. i_S can be regarded as the corrosion rate under the erosion-free condition, so that the corrosion augmentation defined by ASTM G119 is given by

$$\text{Corrosion augmentation} = \frac{\bar{i}}{i_S} = \frac{\dot{c}}{\dot{c}_0} = 1 + \frac{i_1}{i_S}\frac{\lambda_1}{1+\lambda_1} + \frac{i_2}{i_S}\frac{\lambda_2}{1+\lambda_2}. \tag{19}$$

When the repassivation follows the power law, as indicated by carbon steels in the slurries prepared with the borate buffer solution [52, 83]

$$i = i_S + i_{peak}\left(\frac{t}{\tau_0}\right)^{-m}, \quad t > \tau_0, \quad 0 < m < 1. \tag{20}$$

The corrosion current density in flowing slurry and the corrosion augmentation will be formulated as [52]

$$\bar{i} \approx i_S + \frac{i_{peak}}{1-m}\lambda_0^m. \tag{21}$$

$$\text{Corrosion augmentation} \approx 1 + \frac{i_{peak}}{i_S}\frac{\lambda_0^m}{1-m}, \tag{22}$$

where τ_0 and $m\,(0 < m < 1)$ are experimental constants, the non-dimensional parameter $\lambda_0 = \tau_0 \dot{A}_e$. In the practical situations in engineering, $\lambda_0 << 1$. It has been demonstrated that Equation (21) gives good prediction to the corrosion current densities of pipeline steels [52].

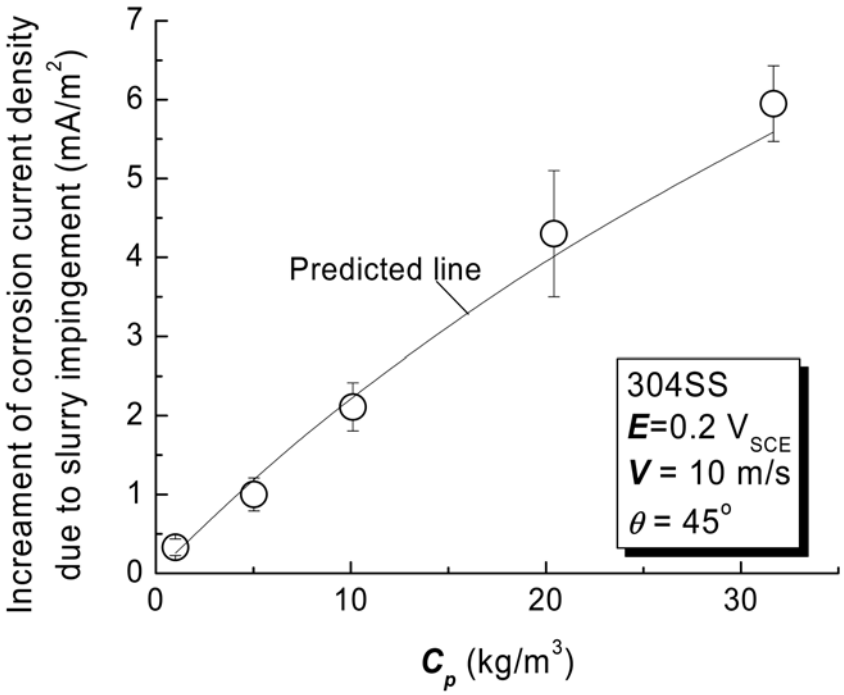

Figure 4. Comparison between theoretical prediction and experimental results of corrosion current density of 304SS under slurry impingement (slurry: tap water + sand, impingement velocity: 5m/s, impingement angle: 45°) [52].

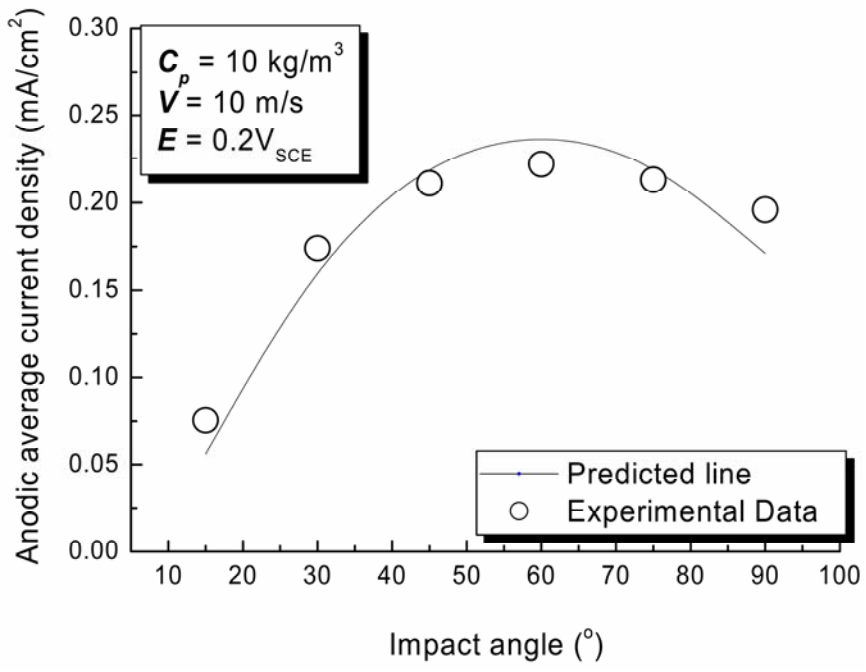

Figure 5. Comparison between theoretical prediction and experimental results of corrosion current density of 304SS under slurry impingement with different impact angles (slurry: tap water + sand, impingement velocity: 5m/s) [85].

4. Erosion and Corrosion-Enhanced Erosion

4.1. Erosion resistance and mechanical properties of target materials

Many mechanical erosion models have been established to correlate the erosion resistance of target materials to their mechanical properties and hydrodynamic parameters [86, 87]. A detailed literature review on this aspect is out of scope of this article. Meng and Ludema [87] provide an exhaustive overview up to 1995, found 182 equations and selected 28 for special study. Lyczkowski and Bouillard [88] gave one up to 2002. As pointed by Tsai et al. [89] over a fairly wide range of variables, at least in flowing slurries, the overall dependence of the particle and target

hardness (H_P and H, respectively), on erosion is approximately given by $\dot{e}_0 \propto H_P^{1/2} / H$. Generally, the erosion resistance of target materials increases with their hardness if no substantial change takes place in the erosion mechanisms and, as illustrated in Figure 6, the power law erosion rate of materials can give a fairly good fit to the correlation between the mechanical erosion rate and surface hardness [4, 7, 90]

$$\dot{e}_0 = \kappa_H H^{-n_H}, \tag{23}$$

where κ_H and $n_H (> 0)$ are experimental constants depending heavily on the erosion mechanisms.

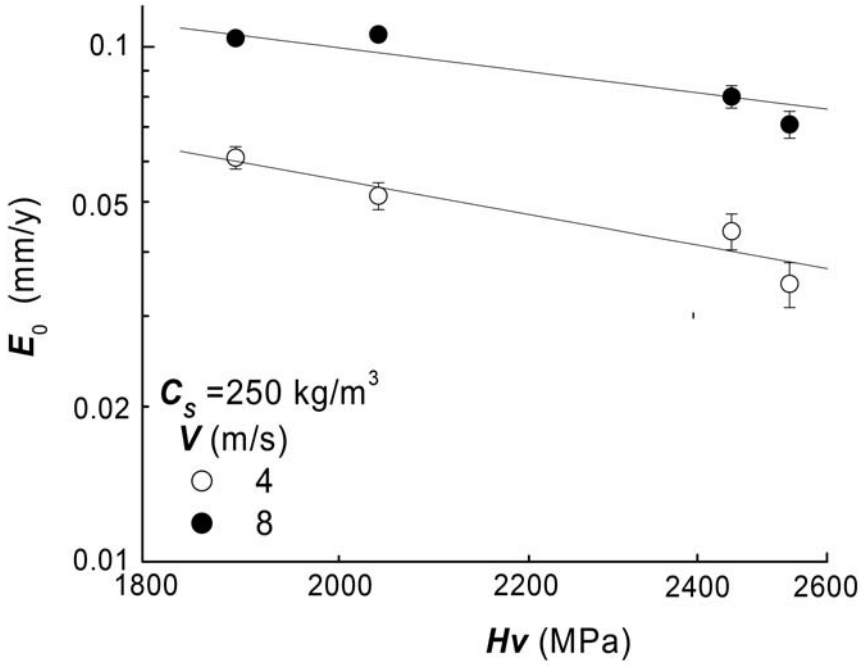

Figure 6. Dependence of erosion rate on the surface hardness [91].

4.2. Corrosion-induced degradation of surface mechanical properties

At least two irreversible processes are involved in the erosion-corrosion process, namely, the electrochemical corrosion at surface and plastic deformation in surface layer. The fluxes of these two irreversible processes can be represented by the corrosion rate $\dot{c}$ (or the anodic current density $i_A = \dot{c} / zF$, where z is the number of electrons involved in the corrosion reaction of the electrode material and F is the Faraday constant) and the plastic strain rate $\dot{\gamma}_P$($= \dot{N}\lambda\overline{b}$, where $\dot{N}$, λ, and $\overline{b}$ are the flux, the mean free path, and Burger's victors of dislocations, respectively). When the anodic dissolution on surface and the plastic deformation in surface layer occurred simultaneously, they will enhance each other leading to the synergistic effect [4, 48, 101],

$$\dot{\gamma}_P = \dot{\gamma}_{P,0} + L_{C\to P}F_C, \tag{24}$$

$$i_A = i_{A,0} + L_{P\to C}F_P, \tag{25}$$

where $\dot{\gamma}_P$ is plastic deformation rate in an inert environment, $i_{A,0}$ is the corrosion current density of material free of dynamic plastic deformation, F_C and F_P are the general driving forces for the plastic deformation (such as the force produced by particle impingement) and anodic dissolution (the potential), respectively, $L_{C\to P}$ and $L_{P\to C}$ are the coefficients representing the cross effects. The second term in Equation (25) stands for the mechanical impact enhanced corrosion [4, 7] and it indicates that the anodic dissolution rate increases linearly with the plastic deformation rate [101, 102]. The second term in Equation (24) implies that the plastic deformation in the surface layer would be promoted by the corrosion occurring on surface. The reduced resistance to the plastic deformation can be characterized by the degradation of surface strength or hardness [4, 48, 101, 92]. The degradation surface hardness due to the presence of anodic dissolution ΔH can be formulated as follows [4]:

$$\frac{\Delta H}{H} = -B \log\left[\frac{i_A}{i_{th}}\right], \tag{26}$$

where H is surface hardness measured in an inert environment, ΔH is defined as the difference between the hardness values measured in corrosive solution, while anodic current is present on surface and in the inert environment. B is a constant related to the active volume of dislocations and test conditions, i_{th} is the threshold current to cause the surface strength degradation. The phenomenon of corrosion-induced surface hardness degradation has been experimentally observed in carbon steels and commercial pure iron by using the microhardness and nanoindentation techniques [4, 48, 101, 92]. An example of corrosion-induced microhardness degradation is demonstrated in Figure 7.

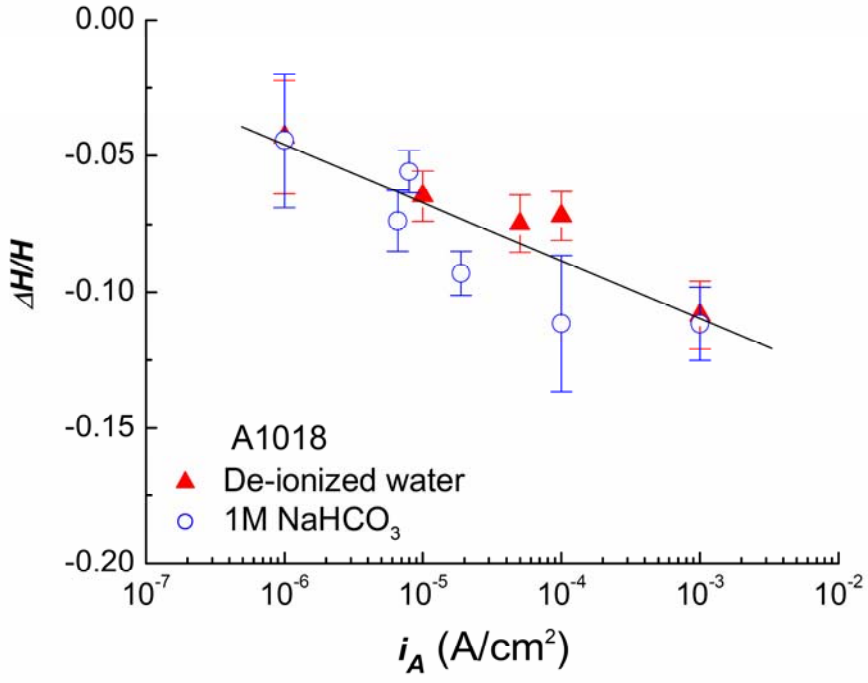

Figure 7. Relationship between the normalized hardness drop and anodic current density [4].

4.3. Corrosion-enhanced erosion

If the increasing erosion rate caused by the anodic dissolution-induced hardness degradation is the only mechanism of corrosion-enhanced erosion, the increment of erosion rate $\Delta\dot{e}$ due to the presence of anodic dissolution can be defined as the corrosion-enhanced erosion, namely, $\dot{e}_c = \Delta\dot{e}_0 = \dot{e} - \dot{e}_0$. By combining Equations (23) and (26), the normalized corrosion-enhanced erosion wastage, i.e., the wastage ratio of $\dot{e}_c / \dot{e}_0$, can be correlated to the anodic current density i_A as follows [4, 48, 101]:

$$\frac{\dot{e}_c}{\dot{e}_0} \approx Z \log\left(\frac{i_A}{i_{th}}\right), \tag{27}$$

where Z is an experimental constant, i_{th} is the threshold anodic current density to cause the corrosion-enhanced erosion. According to Equation (27), the erosion will be enhanced by the chemo-mechanical effect when corrosion occurs simultaneously and the erosion augmentation defined by ASTM G119 $(= 1 + \dot{e}_c / \dot{e}_0)$ will be approximately a linear function of the logarithm of anodic current density. It has been shown the prediction of Equation (27) agrees well with the experimental results obtained of carbon steels, as shown in Figure 8 [4, 48]. The practical engineering, the slurry pipe is normally operated under open circuit potential (OCP). The experiments in [48] indicated that the corrosion-enhanced erosion at the OCP was predictable using the curve obtained under galvanostatic control as the corrosion current density at the OCP is known.

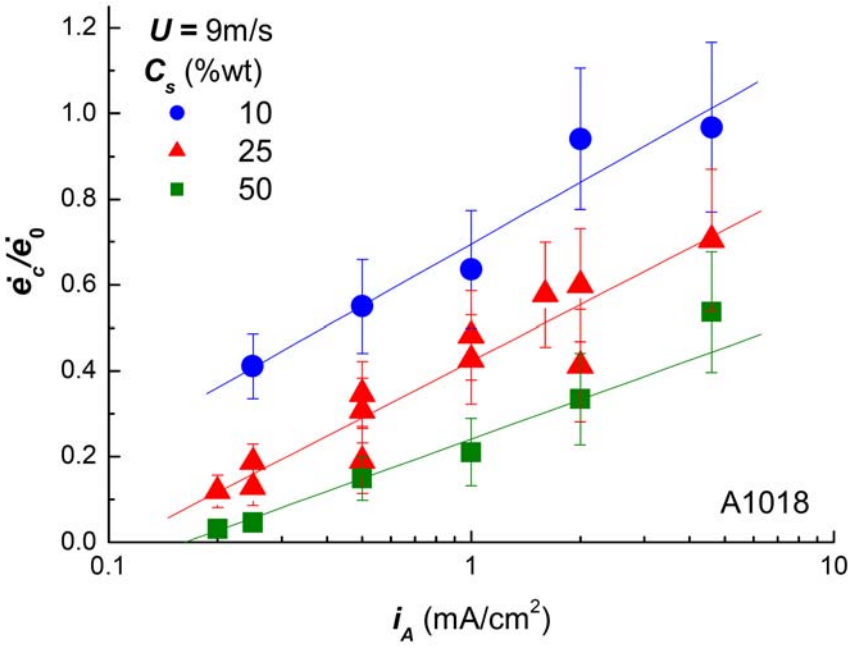

Figure 8. Effect of anodic current density on normalized corrosion-enhanced erosion rate [4, 48].

As shown in Figure 8, the corrosion-enhanced erosion is also affected by the concentration of solid particles in slurry when the anodic current density is held unchanged. The impact the sand concentration can be predicted when the normalized wastage ratio $\dot{c}/\dot{e}_0$ is employed to replace anodic current density, as shown in Figure 9.

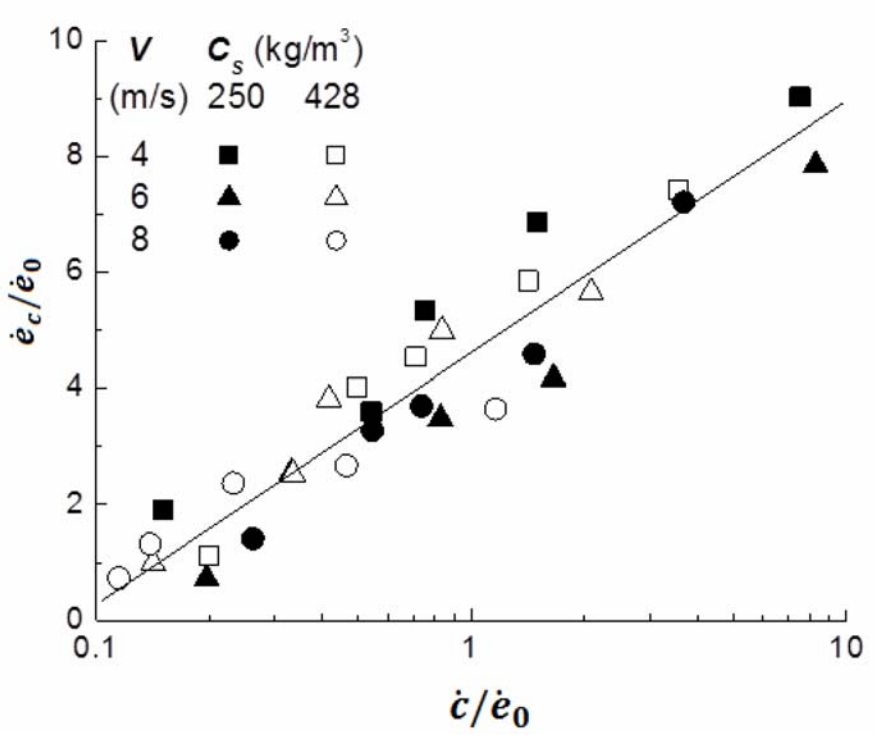

Figure 9. Correlation between normalized mechanical erosion rate and wastage ratio $\dot{c}/\dot{e}_0$ under galvanostatic control [48].

Until now, it is still to build a universal model for the corrosion-enhanced erosion because of complex mechanisms. A recent research [37, 93, 94] indicated that, when the hydrodynamic condition and anodic current density were held unchanged, the erosion rates of carbon steel in acidic slurries were significantly higher than those in alkaline or near-neutral ones. The erosion rates in corroding slurries with high or near-neutral pH were not affected by the slurry chemistry, but the slurry chemistry impact were pronounced in acidic slurries. The high-to-low order of erosion rates were the same as that of in-situ nanoindentation hardness measured in same corroding environments, indicating the anodic dissolution-induced surface hardness degradation as likely the mechanism for the high erosion wastage in acidic slurries. However, it is

still unclear why the exposure to acidic electrolytes results in larger surface hardness loss when anodic dissolution rate is same.

5. Erosion-Corrosion Map

Flowing the concept of 'wear map' developed by Ashby, a group led by Stark [95] built up the erosion-corrosion map to demonstrate that correlation between the erosion-corrosion mechanisms and/or performance of materials and process parameters, such as temperature, potential, flowing velocity, particle concentration, impact angle etc. The erosion-corrosion maps offer a directly perceived illustration about the effects of various parameters on the erosion-corrosion mechanisms and performance of materials. However, there are four different wastage components involved in erosion-corrosion process and so many factors relating to mechanical, chemical, and material aspects that can affect the erosion-corrosion behaviour of material. Besides, the interactions of these factors are very complicated. It is difficult to demonstrate these complex relationships with a few maps. Stark et al. [95, 96] made efforts to group various parameters into dimensionless ones and to build the erosion-corrosion maps by using these dimensionless parameters. However, more work need to be done to understand the physical meanings of these non-dimensional parameters. It is unknown whether or not the erosion-corrosion experimental data from difference sources can be correlated by using these parameters.

6. Prediction of Erosion-Corrosion Rate

Although a lot of efforts have been made to establish a theoretical model that allows us to predict the performance of an engineering components based on the erosion-corrosion experimental data obtained in laboratory, limited progress has been achieved [87, 88, 90]. In practical engineering, the erosion-corrosion rates (ECR) are normally to be correlated to the operating parameters by using empirical equations determined by experiments. An example is as follows [97, 98]:

$$ECR = F_i F_M F_S F_P F_{r/D} \frac{C_P Q_F U_{imp}^{1.73}}{r^2}, \quad (28)$$

where ECR is the penetration rate caused by erosion-corrosion, F_i is inhibitor factor, F_M and F_S, are empirical constants that account for the material hardness and sharpness of sand particles, respectively, F_P is the penetration factor for steel (based on 1" pipe diameter); $F_{r/D}$ is the penetration factor of elbow; C_P is weight fraction of sand; Q_F is the production rate of fluid, r is ratio of pipe diameter in inches to in. pipe; U_{imp} is the characteristic particle impact velocity. The parameters in Equation (27) can be determined by experiments or experience. Generally, the dependence of erosion-corrosion rate on flowing velocity is formulated as follows [6, 99]:

$$ECR = const. \cdot U^{\beta}. \quad (29)$$

The β value depends on the relative contributions of corrosion and erosion to total loss. When the solid erodent is present, the corrosion current density increases with increasing sand concentration [100] and the erosion may dominate the total material wastage. The value of β is often used as a diagnostic tool for the erosion-corrosion mechanism, as summarized in Table 2 [6].

If the solid erodent is present in the electrolyte, the impingement of solid particles can induce the plastic deformation in the surface layer. The anodic dissolution would be promoted by the dynamic plastic deformation. Both theoretical analysis [4, 101] and experimental results [101, 102] indicated that the anodic dissolution current density i_A would increase linearly with the dynamic plastic deformation rate $\dot{\varepsilon}_p$. When the metallic components are exposed to flowing slurry, plastic deformation is induced by the solid particle impingement and the overall plastic deformation rate in surface layer increases with increasing impingement velocity and sand concentration, so that the β-value is likely to be larger than zero even if the corrosion is under the charge transfer control.

Table 2. β value and erosion-corrosion mechanism [6]

Mechanisms of material loss	β
Corrosion	
Liquid-phase mass transfer control	0.8-1
Charge transfer control	0
Mixed charge/mass transfer	0-1
Activation/repassivation	1
Erosion	
Solid-particle impingement	2-3
Liquid droplet impingement in high speed gas flow	5-8
Caviation attack	5-8

In flowing slurries, it is believed that the corrosion is rate-control process, if β is close to 1 and the erosion will dominate the material loss when β is close to 3 [6, 100]. However, a recent study indicated that when the corrosion is controlled by the repeated breakdown of passive films due to particle impingement and repassivation, the β value is close to 3, as shown in Figure 10 [82].

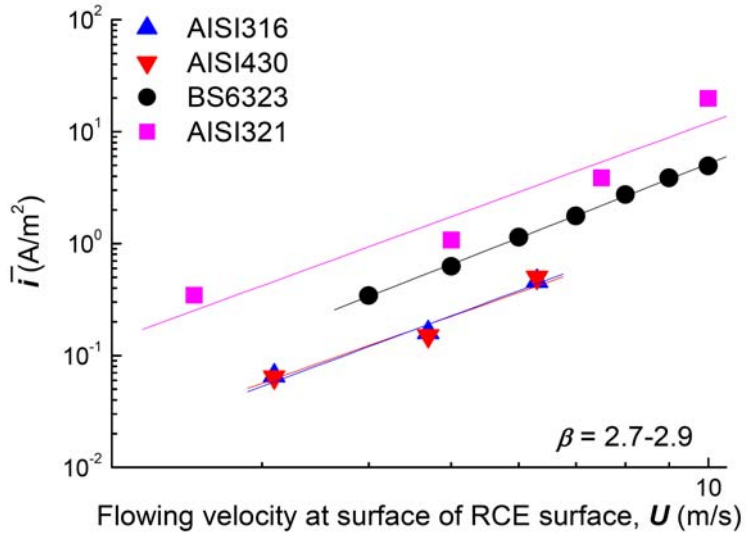

(a)

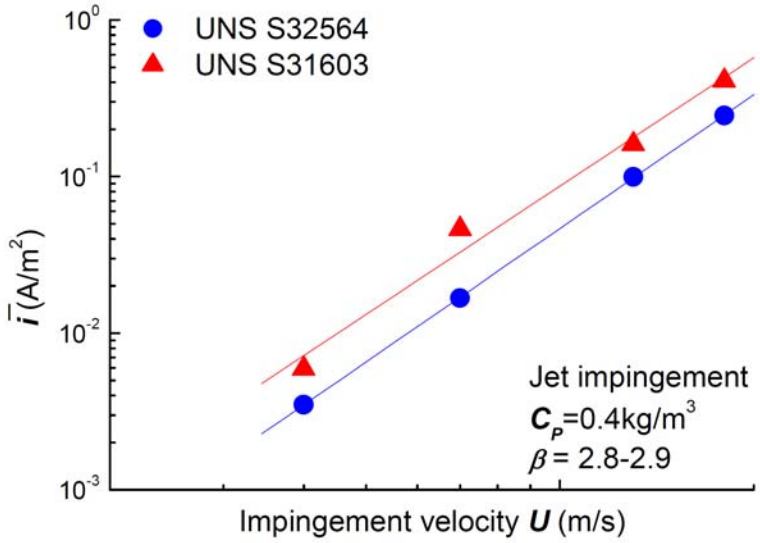

(b)

Figure 10. Dependence of corrosion current densities of passive targets on flowing velocities of slurries: The data measured with (a) rotating cylinder electrode (RCE) system and (b) jet impingement facility [82].

7. Mitigation of Erosion-Corrosion

7.1. Proper design

A careful design of flow geometry can effectively to minimize erosion-corrosion caused by disturbed flow, such as limiting weld root protrusion and steps of fanges [6, 8], utilizing long radius elbows [103], and gradual changes in the flow cross-section [6], replacing the elbow with plugged tee [104]. Utilizing helically-formed pipes to enhance the swirl flow in pipe can reduce the critical flow velocity to suspending solid particles and the erosion rate significantly. The helically-formed pipes can also reduce the pressure drop and improve the particle distribution across the elbow. It leads to erosion uniformly distributed over entire inner pipe surface and hence reduces the potential erosion instead of localized wall penetration [23].

Increasing the thickness of materials in critical areas, using impingement plates to shield the critical areas, and sometimes, rotating pipes can extend the life of tailing lines. In addition, acceptance of a high erosion rate with regular inspection and replacement may be less costly than using more expensive materials is a practice used extensively in minerals processing and oil/gas industries [6].

A proper design also includes optimizing the particle size by grinding and the flow velocity [6], as well as slurry pH and sand control [12]. The erosion rate is reduced significantly when the particle size is less than 100μm [47, 105]. For some geometries where throw sufficient power is possible, cathodic protection is a good option. If the corrosion following the removal of protective film is liquid-phase mass transport controlled, a decrease in flow velocity can retard corrosion process. However, pitting corrosion in flowing slurry has been found in the both field [100] and laboratory tests [62]. The initiation of pitting requires corrosion product layers with local defects [106]. These defects may be the non-uniform growth of the layers and/or to the local mechanical destruction by various fluid-induced mechanical forces. The rupture of protective film results in the rapid anodic dissolution of bare metal in a localized way and, if the repassivation is in any way hindered pits are likely to commence at that

sites. The surface roughness generated by erosion may thus be responsible for the enhanced pitting corrosion during erosion-corrosion, because the rough surface is likely to enhance the localized micro-turbulence [106]. A lower flowing velocity can generally reduce the erosion-corrosion damage and it will reduce the economic output as well [8]. Actually, the flowing velocity cannot be lower than certain limit value to keep particle in suspension [107]. Lower velocities may result in the sliding abrasion of horizontal pipe bottom [6]. Since the localized corrosion will lead a more serious problem than the uniform corrosion, Postlethwaite [108] suggested that slurry pipelines should operate under the conditions that the pipe wall is free from rust and scale to prevent pitting corrosion.

7.2. Material selection

7.2.1. General considerations

In the two-phase liquid/solid flow, the erosion-corrosion performance relies on both the mechanical properties and electrochemical characteristics. Generally, an increase of Cr-content in steels will improve the erosion-corrosion resistance [3, 8]. It has been widely recognized that the erosion resistance of metallic materials increases with increasing relative hardness (the difference between the hardness of target material and particles) [7, 47, 109, 110, 111]. This conclusion is correct only when no substantial change occurs in the erosion mechanism [112, 113]. Finnie [105] reported the erosion rates of annealed metals were inversely proportional to their Vickers hardness, but the erosion rates of some heat-treated steels were almost unaffected by their hardness. Wentzel et al. found that the slurry erosion resistance of white cast irons containing tungsten increases linearly with hardness in the low hardness, but this relationship does not exist in the high hardness range [114]. Finnie attributed this phenomenon to the low strain hardening rates of metallic materials having high yield strength [105]. In the corrosive slurries, the total weight loss caused by slurry erosion, sometimes, does not decrease with increasing hardness of target materials [39, 112]. It has been known the total material loss in corrosive slurry is a sum those caused by erosion

and corrosion, respectively, while the latter does not relate to the hardness of materials. Wang and Stack [115] isolated the corrosion contribution to the total weight loss and found that only the erosion resistance of mild and stainless steels increases with increasing hardness. Sundararajan [116] found that the resistance of metallic, including metallic matrix composites (MMCs), against the erosion caused by solid/gas mixture was often not well correlated to the mechanical properties measured under quasi-static loading conditions. He suggested using the dynamic hardness in evaluating the erosion resistance [116]. Although, attempts have been made, it is still hard to generalize the effects of hardness [47, 105, 117]. As pointed by Kato [117], the wear resistance is not only dependent on hardness, but also on the ductility of material, as well as surface roughness.

Actually, the correlation between the erosion resistance and hardness of base metal depends on the erosion mechanism. Heitz [66] pointed out that, if the mechanical damage is restricted in the surface layer, especially in corrosion product scale or passive film, it normally exists in the single-phase flow, the adherence, cohesion, and hardness of surface layer determines mechanical stability. In this case, the hardness of base metal is not relevant to the erosion-corrosion process, but certain chemical changes in these layers may be the cause of a breakdown with subsequent onset of erosion-corrosion. In many corrosion systems, a protective film is likely to form on a metal surface when it exposes to its environment and the film plays an important role in the erosion-corrosion mechanism of materials. The passive film has an ability to inhibit erosion-corrosion damage to a certain extent through inhibiting corrosion as long as it is chemically stable in the environment [118]. The protective function of film relates to its formation kinetics, mechanical properties, and hydrodynamic conditions of fluid [119, 120, 121, 122]. The kinetics of film formation depends on the composition of materials and conditions of environment [118, 123]. For a ferrous alloy, the protective ability of the film increases with increasing chromium concentration in a matrix [123].

7.2.2. Steels

As is summarized by Finner et al. in 1967 [124], for example, erosion rate tends to increase with reduced hardness for pure metals but not for steels. Hutchings [125] proposed to correlate the erosion rate to the microhardness of steels measured on the eroded surface. An alternative explanation is the high strain rate created by solid particle impingement may play a role, so that the erosion models based on the dynamic hardness were proposed [126, 127]. The impingement velocity of particles during slurry erosion is relatively low. Lu et al. [4, 48] found the erosion rate was reduced with increasing hardness of carbon steels. Wood [7] reported slurry erosion rates measured from metallic and ceramic materials and found that the erosion rate was reduced with increasing hardness and erosion, no matter the materials were brittle or ductile. The corrosion-enhanced erosion is also affected by the corrosion mechanism. The experimental evidences have indicated that the erosion resistance of carbon steels increases with increasing carbon content in composition [111, 128]. Steels with low-bainitic structure are generally more resistant to erosion-corrosion than those have ferrite + pearlite structure [129].

High chrome cast steels are more resistant to erosion-corrosion than plain cast iron and this attributes to its higher Cr concentration in matrix and martensitic structure [130]. Generally, the erosion-corrosion resistance of steels increases with increasing chromium concentration in matrix. Therefore, stainless steels are more resistant to erosion-corrosion than carbon and low alloy steels, while the erosion-corrosion resistance of austenitic stainless steels is better than ferritic stainless steels [115, 131]. Experimental data indicate that addition of alloy elements Cr, Mo, Mn, N would improve the erosion-corrosion resistance of stainless steels [132, 133, 134].

Lindsley et al. [135] investigated the erosion resistance and morphology of spheroidized Fe-C alloys with various carbon content and microstructure, and they found that the erosion resistance increased as

the mean free path between both the grain boundaries and the carbides decreases. Same phenomenon has been also reported in ferrous alloys containing 0.4 to 1.4%C [135]. These variables control dislocation motion in the ferrite and, in turn, affect the plastic deformation and the erosion resistance of materials. A Hall-Petch-type relationship was found between the mean free path of microstructure and both erosion rate and hardness [135].

7.2.3. Chrome white irons

Chrome white irons (CWIs) are specifically developed for abrasion resistant applications [136], because of their excellent abrasive resistance and moderate ability against impact, which necessary for crushing, grinding, and slurry erosion applications [44, 137, 138]. It is often applied as weld hardfacing alloy deposited on the surface of low carbon steel pipelines to improve the erosion-corrosion resistance steel pipes [139]. Generally, high carbon content is required for the formation of carbides to provide erosion resistance [138, 140], but the chromium content in matrix is critical to the corrosion resistance of material [112, 141, 142]. The optimum C content appeared to depend on the Si level [142]. Dodd pointed out the alloys contained 2-2.5%C, 20-28%Cr with 2%Mo have good resistance to erosion-corrosion at pH values down to 4. A part of chromium is consumed in the formation of carbides. The experimental evidence has indicated that the minimum Cr content in matrix is 12%. Based on the distribution of Cr between the matrix and carbides determined by electronic probe [143] and the experimental results of dry sand wear and corrosion. Lu et al. [112] establish the wear-and corrosion performance map of chrome white iron, as shown in Figure 11.

However, the erosion-corrosion resistance of chrome white irons depends heavily on the morphology, distribution, and size of the secondary phase, as well as erosion mechanism [44, 112, 144, 145]. The matrix structure is adjusted by heat treatment and alloy content to balance wear properties and toughness [136, 146]. The effect of

microstructure on corrosion resistance is still unclear [147, 148]. The slurries in the oil sand production are often corrosive. CWIs become less resistant to wear when corrosion is present [28, 149]. When chrome white iron was eroded in slurry with low pH, the contribution of synergism to total material loss was reported being as high as 86.3% [28]. Therefore, a comprehensive understanding of mechanisms of synergistic effect is critical to improve the erosion resistance in corrosive media.

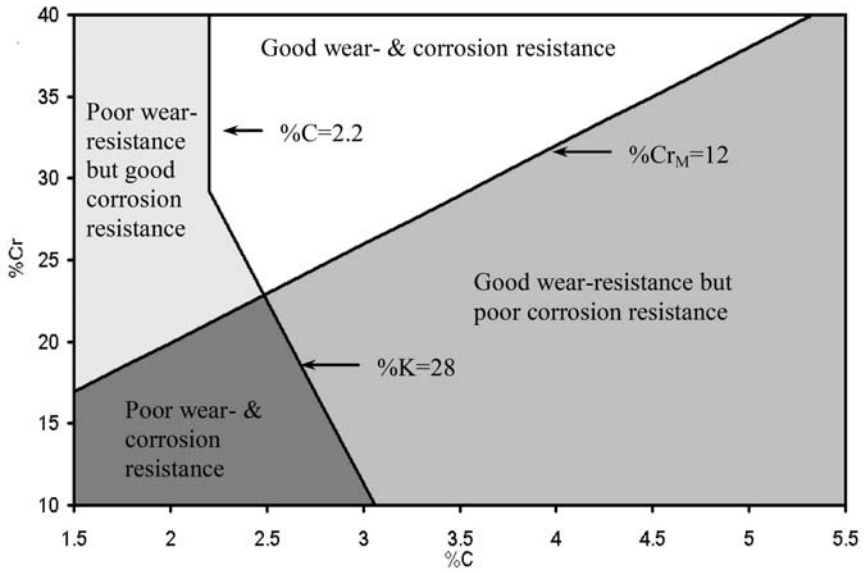

Figure 11. Wear/corrosion performance map of chrome white irons [112].

7.2.4. Metal matrix composites

The metal matrix composites (MMCs) comprise metallic binder and hard particles phases, and they are normally used as hard coating. The binder materials include Ni, Co, Al and their alloys [150, 151, 152]. Sometimes, austenitic stainless steel was also adopted [153]. The hard particles commonly used include WC, B_4C, and SiC. Scanning electron microscopic (SEM) study confirmed that wear of composite is mainly governed by the synergistic effect of the two simultaneous processes: (1) corrosion, erosion, and abrasion of the matrix by the slurry; and (2)

fracture and removal of the hard particles due to erodent impingement at a high speed [150, 151, 154]. The erosion-corrosion resistance of MMC depends heavily on the corrosion resistance of binder, since the binder material tends to dissolve preferably. The hard particles will be readily removed by erosion if they loss support of binder [39, 150, 156]. The differences in binder composition will influence the MMCs' hardness and corrosion behaviour, which in turn affects the synergistic action of erosion-corrosion. The erosion-corrosion mechanism depends heavily upon the corrosion kinetics of binder [150, 152] and mechanical properties of hard particles [155]. The inherent corrosion resistance of pure nickel and cobalt binder did not increase the erosion-corrosion resistance of the MMCs in slurry, but both the nickel-chromium-cobalt grades and the nickel-chromium grades were found to improve the erosion-corrosion behaviour compared to the pure cobalt grade [152, 156]. This result indicates that the erosion-corrosion resistance of MMC can be further improved by optimizing the binder composition.

The performance of MMCs is closely related to the corrosion kinetics of binder [150, 152], as well as the volume fraction and mechanical properties of hard particles [157]. Pugsley et al. [158] investigated the cavitation erosion performance of a range of tungsten carbide-cobalt (WC-Co) composites of various grain sizes ($0.5 \sim 5\mu m$) and cobalt contents ($6 \sim 15\%wt$). They found that the correlation of the erosion-corrosion resistance and the binder content depended on the erosion-corrosion mechanism, while the WC gain size is of strong influence on the erosion-corrosion mechanism. The interface structure between the hard particles and matrix can affect the erosion-corrosion resistance significantly [153]. The surface analysis has indicated that the performance of WC-Co-Cr system can suffer localized corrosion in area adjacent to the interface of particle/matrix [159].

7.3. Application of coating and surface hardening techniques

Coating techniques play an important role in minimizing the loss caused by erosion-corrosion. The CWIs and MMCs are most commonly used coating materials. WC and W_2C are almost as hard as diamond.

They are particularly suitable to be used in hardfacing. Tungsten carbide overlay coatings can be applied by high-velocity oxygen fuel spraying (HVOF) or welding. The coating thickness obtained by HVOF technique is between 10 to 1000mm, which is suitable for the valves, pistons, and pump impellers. The extremely abrasive conditions in oil drilling demand thicker coatings and better bonding. The plasma-transferred arc (PTA) process using multilayer technique can produce facings up to 120mm. It is widely used in equipments for oil extraction in oil sand industry in Canada [160]. Other coatings processes, involving chemical vapour deposition, have been used to produce ultra-hard coatings like diamond for pump components and mechanical seals [7]. As a low cost approach to improve the surface hardness of steel pipe, induction-quenching technique was utilized to improve the internal pipe surface. However, the process parameters are still needed to be optimized to prevent pitting corrosion caused by the heterogeneity of microstructure [161].

7.4. Application of inhibitor and chemical control

In many cases, it is technically difficult to change the nature of slurry to be transported. According to the understanding of damage mechanisms resulting from the synergism of mechanical and (electro) chemical factors, as those described in the previous sections, the material performance can be improved by reducing corrosion rate.

The addition of inhibitor could efficiently reduce the corrosion and corrosion-enhanced erosion wastages of carbon steel in slurry containing 1% silica sand and saturated with CO_2 [16]. Chromates and nitrites with high concentrations act as passivating inhibitors, whereas chromates at low concentration act as a cathodic inhibitor, and were used in the first long distance coal-slurry pipelines [162, 163]. However, chromates are highly toxic, so that effort have been made to find non-chromate inhibitors used in the cooling water systems, zinc, sodium tripolyphosphate ($Na_5P_3O_{10}$), and nitrilotris (methylene) triphosphonic acid $N[CH_2PO(OH)_2]_3$, showed little benefit in erosive slurries when used alone or along with chromates [6].

Solution conditioning involves raising the pH and/or deaeration, as illustrated in Figure 9. Both have been applied to long-distance slurry pipelines. An increase in pH can promote pitting because thicker scale is likely to form [164, 165]. Deaeration is achieved by adding oxygen scavengers, such as bissulphite or hydrazine, or by non-chemical steam stripping or vacuum deaeration. The latter two methods of deaeration are not suitable for slurry pipelines. They are used extensively with oil-well water injection systems [166].

8. Summary

Erosion-corrosion is big concern in oil and gas production. Although significant efforts have been made, it is still difficult to evaluate the erosion-corrosion wastage of engineering materials and/or components in a quantitative way, because of the complexity resulting form the synergisms among the factors relating to mechanics, chemistry, and materials. The economic loss due to erosion-corrosion can be minimized by utilizing proper design, material selection, and chemical control.

References

[1] J. Postlethwaite, M. H. Dobbin and K. Bergevin, Corrosion 42 (1986), 514-524.

[2] G. T. Burstein and K. Sasaki, Electrochim. Acta 46 (2001), 3675-3683.

[3] B. Poulson, Corrosion Science 23(4) (1983), 391-430.

[4] B. T. Lu and J. L. Luo, J. Phys. Chem. B 110 (2006), 4217-4231.

[5] ASTM G15-05, Standard Terminology Relating to Corrosion and Corrosion Testing, Annual Book of ASTM Standards, Vol. 03.02, Wear and Erosion, Metal Corrosion, West Conshohocken, PA, (2005), 65-68.

[6] J. Postlethwaite and S. Nesic, Erosion-Corrosion in Single and Multiphase Flow, Uhlig's Handbook, 2nd Edition by W. Revie, John Wiley & Sons, Inc., (2000), 249-272.

[7] R. J. K. Wood, Wear 261 (2006), 1012-1023.

[8] P. B. Poulson, Erosion-Corrosion, in Corrosion, L. L. Shreir, R. A. Jarman, G. T. Burstein, (ed.) \ 3rd Edition, Elsevier, (1994), 293-303.

[9] K. D. Efird, Corrosion 2000, Paper No. 52, NACE International, Huston, TX, 2000.

[10] I. Owen and J. Madadnia, ASME, Fluids Engineering Division, (Publication), V. 226, Cavitation and Gas-Liquid Flow in Fluid Machinery and Devicesm (1995), 59-62.

[11] K. T. Kembaiyan and K. Keshavan, Wear 186-187 (1995), 487-492.

[12] R. Hamzah, D. J. Stephenson and J. E. Strutt, Wear 186-1987 (1995), 493-496.

[13] A. Procyk, M. Whitelock and S. Ali, Oil & Gas Journal (1998), 80-90.

[14] P. Andrews, T. F. Illson and S. J. Mathews, Wear 233-235 (1999), 568-574.

[15] H. M. Clark and R. J. Lwellyn, Wear 250 (2003), 206-218.

[16] C. Wang, A. Neville, S. Ramachandran and V. Jovancicevic, Wear 258 (2005), 649-658.

[17] J. R. Shaley, S. A. Shirazi, E. Dayalan and E. F. Rybicki, Corrosion 54 (1998), 972-978.

[18] D. Raghu, B. McKee, C. Sheriff and J. B. C. Wu, Corrosion'01, Paper No. 513, NACE International, TX, USA, 2001.

[19] R. D. Kane and M. S. Cayard, Corrosion'02, Paper No. 555, NACE International, Houston, TX, USA, 2002. `

[20] Z. Klenowicz, K. Darowicki, S. Krakowiak and A. Krakowiak, Mater. Corr. 54 (2003), 181-187.

[21] X. Q. Wu, H. M. Jing, Y. G. Zheng, Z. M. Yao and W. Ke, Wear 256 (2004), 134-141.

[22] P. McLintyre, Marine Corrosion Club Meeting, Aberdeen, 1999.

[23] R. J. K. Wood, T. F. Jones, N. J. Miles and J. Ganeshalingam, Wear 250 (2001), 770-778.

[24] B. Poulson, Wear 233-235 (1999), 497-405.

[25] A. Neville, T. Hodgkiess and J. T. Dallas, Wear 186-187 (1995), 497-507.

[26] M. Matsumura and Y. Oka, Slurry Erosion-Corrosion on Commercial Pure Iron in Fountain-Jet Facility, Proc. 7th Int. Conf. on Erosion by Liquid and Solid Impact, Cambridge, UK, Cavendish Lab. University of Cambridge, (1987), 40.

[27] X. Hu and A. Neville, Wear 258 (2005), 641-648.

[28] Z. Yue, P. Zhou and J. Shi, Wear of Materials, (ASME, New York, 1987), 763-771.

[29] B. W. Madson, Wear 123 (1988), 127-142.

[30] C. H. Pitt and Y. M. Chang, Corrosion 42 (1986), 312-317.

[31] ASTM G119-04, Standard Guide for Determining Synergism between Wear and Corrosion, West Conshohocken, PA, (2006), 519-523.

[32] S. W. Watson, F. J. Friederdorf, B. W. Madson and S. D. Cramer, Wear 181-183 (1995), 476-484.

[33] M. M. Stack, International Materials Reviews 50 (2005), 1.

[34] B. W. Madson, Wear 123 (1988), 127-136.

[35] ASTM G59-97, Conducting Potentiodynamic Polarization Resistance Measurement, West Conshohocken, PA, (2005), 519-523.

[36] ASTM G5-94, Making Potentiostatic and Potentiodynamic Anodic Polarization Measurements, West Conshohocken, PA, 1994.

[37] B. T. Lu, K. Wang, X. M. Wan and J. L. Luo, Degradations of Mechanical Properties in Surface Layer and Erosion Resistance of Carbon Steel in Slurries with Different pH and Chemical Compositions, in this Conference, 2008, Submitted to Corrosion, 2008.

[38] J. Postlethwaite, Corrosion 37 (1981), 1-5.

[39] A. Neville and X. Hu, Wear 250-251 (2001), 1284-1294.

[40] Y. Li, G. T. Burstein and I. M. Hutchings, Wear 186-187 (1995), 515-522.

[41] P. Christodoulou, A. Drotlew and W. Gutowski, Wear 211 (1997), 129.

[42] V. A. Pugsley and C. Allen, Wear 233-235 (1999), 93.

[43] M. C. Wang, S. Z. Ren, X. B. Wang and S. Z. Li, Wear 160 (1993), 259.

[44] X. Huang and Y. Wu, J. Mater. Eng. Perform. 7 (1998), 463.

[45] H. M. Clark, Wear 152 (1992), 223-240.

[46] W. Blatt, W. Kohloey, U. Lotz and E. Heitz, Corrosion 45 (1989), 793.

[47] I. M. Hutchings, The Erosion of Materials by Liquid Flow, MTI Publication No. 25, Materials Technology Institute of the Chemical Process Industries, Inc., 1986.

[48] B. T. Lu, J. F. Lu and J. L. Luo, Corros. Sci. 53 (2011), 1000-1008.

[49] M. Bjordal, E. Bardal, T. Rogne and T. G. Eggen, Surface and Coatings Technology 70 (1005), 215.

[50] S. Das, D. P. Mondal, O. P. Modi and R. Dasgupta, Wear 231 (1999), 195.

[51] B. K. Prasad, Wear 238 (2000), 151.

[52] B. T. Lu and J. L. Luo, Electrochimica Acta 53 (2008), 7022-7031.

[53] A. Neville and T. Hodgkiess, British Corrosion Journal 32 (1997), 197.

[54] B. Poulson, Corrosion Science 23 (1983), 391.

[55] ASTM G76-05, Standard Test Method for Conducting Erosion Tests by Solid Particle Impingement Using Gas Jet, West Conshohocken, PA, (2006), 310-315.

[56] ASTM G134-95, Standard Test Method for Erosion of Solid Materials by a Cavitating Liquid Jet, West Conshohocken, PA, (2006), 559-571.

[57] ASTM G72-04, Standard Practice for Liquid Impingement Erosion Testing, West Conshohocken, PA, (2006), 273-290.

[58] D. C. Silverman, Corrosion 60 (2004), 1003-1024.

[59] J. Postlethwaite, M. H. Dobbin and K. Bergevin, Corrosion 42 (1986), 514-521.

[60] T. V. Chen, A. A. Moccari and D. D. Mcdonald, Corrosion 48 (1992), 239-255.

[61] B. Poulson, Corrosion Science 23 (1983), 391-430.

[62] E. Heitz, Corrosion 47 (1991), 135-145.

[63] J. S. Newman and K. E. Thomas-Alyea, Electrochemical Systems, Wiley-IEEE, (2004), 378-400.

[64] B. Poulson, Corrosion Science 30 (1990), 743-746.

[65] C. W. Chen. T. Yu, B. T. Lu and J. L. Luo, Corrosion during Waster Slurry Transportation.

[66] E. Heitz, Corrosion 47 (1991), 135-145.

[67] D. D. Mcdonald, J. Electrochem. Soc. 196 (1992), 3434-3449.

[68] S. Sikora, J. Sikora and D. D. Mcdonald, Electrochim. Acta 41 (1996), 783.

[69] P. Andrews, I. F. Illson and S. J. Mathews, Wear 233-235 (1999), 568-574.

[70] API RP 14E: Recommended Practice for Design and Installation of Offshore Production Platform Piping System, Washington DC, API, 1991.

[71] B. D. Craig, Mater. Perform. (1998), 59-60.

[72] M. Seo and M. Chiba, Electrochimica Acta 47 (2001), 319-325.

[73] ASM Metals Handbook, 13, 624, ASM Metals Park, Ohio, 1981.

[74] K. D. Efird, Corrosion 33 (1976), 3.

[75] V. L. Streeter, E. B. Wylie and K. W. Bedford, Fluid Mechanics, 9th Edition, McGraw-Hill, New York, 291 (1998m), 105.

[76] R. H. Perry and D. Green, Editors, Perry's Chemical Engineers' Handbook, 7th Edition, McGraw-Hill, New York, (1998), 6-10.

[77] G. Schmitt, C. Werner and M. J. Schoning, Corrosion'02, Paper No. 280, NACE International, TX, USA, 2002.

[78] B. C. Syrett, Corrosion 32 (1975), 242.

[79] B. T. Lu and J. L. Luo, Electrochimica Acta 56 (2010), 559-565.

[80] H. X. Guo, B. T. Lu and J. L. Luo, Electrochimica Acta 51 (2006), 5341-5348.

[81] K. Sasaki and G. T. Burstein, Philosophical Magazine Letters 80 (2000), 489-493.

[82] B. T. Lu, J. L. Luo and H. Y. Ma, J. Electrochem. Soc. 154 (2007), C159-C168.

[83] R. W. Staehle, Corrosion Science 49 (2007), 7-19.

[84] R. Oltra, B. Chapey and L. Renaud, Wear 186-187 (1995), 533.

[85] B . T. Lu, L. C. Mao and J. L. Luo, Electrochimica Acta 56 (2010), 85-95.

[86] A. Levy, Gas-Solid Particle Erosion and Erosion-Corrosion of Metals, Uhlig's Handbook, 2nd Edition by W. Revie, John Wiley & Sons, Inc., (2000), 273-293.

[87] H. C. Meng and K. C. Ludema, Wear 181-183 (1995), 443-457.

[88] R. W. Lyczkowski and J. Bouillard, Progress in Energy and Combustion Science 28 (2002), 543-602.

[89] W. Tsai, J. A. C. Humphrey, I. Cornet and A. Levy, Wear 68 (1981), 289-303.

[90] G. Sundararajan, Wear 186-187 (1995), 129-144.

[91] B. T. Lu, J. F. Lu and J. L. Luo, Corros. Sci. 53 (2011), 1000-1008.

[92] H. X. Guo, B. T. Lu and J. L. Luo, Electrochimica Acta 51 (2005), 315-323.

[93] K. Wang, B. T. Lu, X. M. Wan and J. L. Luo, Canadian Metallurgical Quarterly 50 (2011), 181-185.

[94] B. T. Lu, K. Wang, X. M. Wan and J. L. Luo, Correlation between Degradations of Mechanical Properties in Surface Layer and Erosion Resistance of Carbon Steel-Effects of Slurry Chemistry, Tribology International, 2012, in Revision.

[95] M. M. Stark, Intern. Mater. Rev. 50 (2005), 1-17.

[96] M. M. Stark, N. Corlett and S. Turgoose, Wear 233-235 (1999), 535-541.

[97] J. Jordan, Corrosion'98, Paper No. 59, NACE International, Houston, TX, New York, 1998.

[98] B. S. McLaurym, S. A. Shirazi, J. R. Shadley and E. F. Rybiscki, Corrosion'99, Paper No. 34, NACE International, Houston, TX, New York, 1999.

[99] U. Lotz, Corrosion'90, Paper No. 27, NACE International, Houston, TX, New York, 1990.

[100] J. S. Shadley, S. A. Shirazi, E. Dayalan, M. Ismail and E. F. Rybiscki, Corrosion 52 (1996), 714-723.

[101] G. M. Gutman, Mechanochemistry of Materials, Cambridge Intern. Sci. Publ., Great Abington, Cambridge, UK, 1998.

[102] R. G. Raicheff, A. Damajanovic and J. O. M. Bockris, J. Chemical Physics 47 (1967), 2198-2217.

[103] J. Wang and S. A. Shirazi, ASME J. Energy Res. Tech. 125 (2003), 21-34.

[104] X. Cheng, B. S. McLaurym and S. A. Shirazi, Wear 261 (2006), 715-722.

[105] I. Finnie, Wear 186-187 (1995), 1-10.

[106] G. Schmitt, P. Bosch, P. Plagemann and K. Moeller, Corrosion'02, Paper No. 244, NACE International, 2002.

[107] J. Postlethwaite, B. J. Brandy, M. W. Hawrylak and E. B. Tinker, Corrosion 34 (1978), 245.

[108] J. Postlethwaite, J. Materials Performance 26 (1987), 41-45.

[109] S. Aso, S. Goto, Y. Komatsu, W. Liu and M. Liu, Wear 233-235 (1999), 160-167.

[110] N. J. G. Chacon and F. H. Stott, Corrosion Science 35 (1993), 1045-1051.

[111] R. Dasgupta, B. K. Prasad, A. K. Jha, O. P. Modi, S. Das and A. H. Yegneswaran, Wear 213 (1997), 41-46.

[112] C. Allen and A. Ball, Tribology Intern. 29 (1996), 105-116.

[113] B. T. Lu, J. L. Luo and S. Chiovelli, Mater. Trans. A 37A (2006), 2029-2038.

[114] E. J. Wentzel and C. Allen, Intern. J. Refractory Metals and Hard Materials 15 (1997), 81-87.

[115] H. W. Wang and M. M. Stark, J. Materials Science 38 (2000), 5263-5273.

[116] G. Sundararajan, Wear 186-187 (1995), 129-144.

[117] K. Kato, Wear 241 (2000), 151-157.

[118] M. Matsumura, Y. Oka, Y. Hiura and M. Yano, ISI J. Int. 31 (1991), 168-176.

[119] T. A. Adlerm and R. P. Walters, Wear 162-164 (1993), 713-720.

[120] D. Li, X. Mao and R. Zhu, Corrosion 49 (1993), 877-884.

[121] Z. M. Yao and A. Bronson, Corrosion 49 (1993), 479-485.

[122] P. D. Bastek, R. C. Newmann and R. G. Kelly, 140 (1993), 1886-1889.

[123] T. G. Gooch, Welding Journal 75 (1996), 135/s-154/s.

[124] I. Finner, J. Wolak and Y. Kabil, J. Mater. 2 (1967), 682-700.

[125] I. M. Hutchings, Tribology, Friction and Wear of Engineering Material (1992), Edward Arnord.

[126] I. M. Hutchings, Wear 70 (1981), 688-695.

[127] Y. I. Oka, M. Matsumura and T. Kawabata, Wear 162-164 (1993), 688-695.

[128] B. W. Madson, Wear of Materials, ASME, New York, (1985), 345-354.

[129] B. Q. Wang, G. Q. Geng and A. V. Levy, Wear 151 (1991), 351-364.

[130] W. A. Metwally and M. K. Samy, Steel Research 65 (1994), 455-458.

[131] A. Neville, T. Hodgkiess and J. T. Dallas, Wear 186-187 (1995), 497-507.

[132] J. D. Majumdar and I. Manna, Mater. Sci. Eng. A 267A (1999), 50-59.

[133] D. J. Mills and R. D. Knutsen, Wear 215 (1998), 83-90.

[134] A. Toro, A. Sinatora, D. K. Tanaka and A. P. Tschiptschin, Wear 215 (2001), 1257-1264.

[135] B. A. Lindsley and A. R. Marder, Metall. Mater. Trans. A 29A (1998), 1071-1079.

[136] C. P. Tabrett, I. R. Sare and M. R. Ghomashchi, Inter. Mater. Rev. 41 (1996), 59-82.

[137] T. A. Adler and O. N. Dogan, Wear 225-229 (1999), 174-180.

[138] B. F. Levin, J. N. DuPont and A. R. Marder, Wear 181-183 (1995), 810-820.

[139] S. G. Sapate, A. V. R. Rao and N. K. Garg, Mater. Manufact. Process. 15 (2000), 747-759.

[140] T. A. Adler and O. N. Dogan, Wear 223-229 (1999), 174-180.

[141] J. Dodd, High-Chromium Cast Irons, Corrosion 3rd Edition, L. L. Shreir, R. A. Jarman and G. T. Burstein, Butterworth-Heinemann, Oxford, UK, (1994), 138-137.

[142] P. Christodoulou, A. Drotlew and W. Gutowski, Wear 211 (1997), 129-133.

[143] G. Laird, II, Trans. American Foundrymen's Society 99 (1991), 339-357; 102 (1994), 497-504.

[144] S. Seetharamu, P. Sampathkumaran and R. K. Kumar, Wear 186-187 (1995), 159-167.

[145] Z. Ren, Z. Xuan and D. Sun, Weld. Res. Abroad 47 (2001), 18-23.

[146] R. S. Jackson, J. Iron & Steel Inst. 208 (1970), 163-167.

[147] A. K. Patwardhan and N. C. Jain, Metall. Trans. A 22A (1991), 1991-2319.

[148] V. Kumar and A. K. Patwardhan, Mater. Perform. (1993), 66-69.

[149] L. Valentinelli, T. Valente, F. Casadei and L. Fedrizzi, Corrosion Engineering Science and Technology 39 (2004), 301-307.

[150] Y. l. Saraswashi, S. Das and D. P. Mondal, Mater. Sci. Eng. A 425 (2006), 244-254.

[151] A. Neville, F. Reza, S. Chiovelli and T. Revega, Corrosion 62 (2006), 657-675.

[152] M. Bjordal, E. Bardal, T. Rogne and T. G. Eggen, Wear 186-187 (1995), 508-514.

[153] Y. Gao, F. Zhang, J. Xing, W. Tang and C. Bao, Journal of Xi'an Jiaotong University 35 (2001), 727-730.

[154] S. Das, D. P. Mondal, O. P. Modi and R. Dasgupta, Wear 231 (1999), 195-205.

[155] R. Colaco and R. Vilar, Wear 254 (2003), 625-634.

[156] A. Neville, M. Reys, T. Hodgkiess and A. Gledhill, Wear 238 (2000), 138-150.

[157] R. Colaco and R. Vilar, Wear 254 (2003), 625-634.

[158] V. A. Pugsley and C. Allen, Wear 233-235 (1999), 93-103.

[159] R. J. K. Wood, J. Phys. D. Appl. Phys. 40 (2007), 5502-5521.

[160] U. Morkrmer, R. F. Moll and M. Oechsle, Sultzer Technical Review 3-5 (2005), 12-14.

[161] B. T. Lu, W. S. Li, J. L. Luo and S. Chiovelli, J. Mater. Sci. (2012), 6823-6834.

[162] J. Postlethwaite, Corrosion 35 (1987), 475; 31 (1981), 1.

[163] J. Postlethwaite, Mater. Perform. 26 (1987), 41.

[164] M. E. Jenning, Mining Eng. (1981), 178.

[165] R. D. Colale, T. L. Thompson and R. P. Ehrlich, Trans. SME, AIME 260 (1976), 289.

[166] A. G. Osstroff, Introduction to Oilfield Water Technology, NACE, Houston, TX, (1979), 293.

■